DOI: 10.4046/trd.2011.70.5.397
ISSN: 1738-3536(Print)/2005-6184(Online)
Tuberc Respir Dis 2011;70:397-404

Original Article

Pandemic Influenza A/H1N1 Viral Pneumonia without Co-Infection in Korea: Chest CT Findings

Jun Seong Son, Ph.D.[1], Yee Hyung Kim, M.D.[2], Young Kyung Lee, M.D.[3], So Young Park, M.D.[4], Cheon Woong Choi, Ph.D.[2], Myung Jae Park, Ph.D.[4], Jee-Hong Yoo, Ph.D.[2], Hong Mo Kang, M.D.[4], Jong Hoo Lee, M.D.[5], Boram Park, M.D.[6]

Departments of [1]Infectious Diseases, [2]Pulmonary and Critical Care Medicine, and [3]Radiology, Kyung Hee University Hospital at Gangdong, School of Medicine, Kyung Hee University, [4]Department of Pulmonary and Critical Care Medicine, Kyung Hee Medical Center, School of Medicine, Kyung Hee University, Seoul, [5]Department of Pulmonary and Critical Care Medicine, Jeju National University Hospital, Jeju, [6]Graduate School, Kyung Hee University, Seoul, Korea

Background: To evaluate chest CT findings of pandemic influenza A/H1N1 pneumonia without co-infection.
Methods: Among 56 patients diagnosed with pandemic influenza A/H1N1 pneumonia, chest CT was obtained in 22 between October 2009 and Februrary 2010. Since two patients were co-infected with bacteria, the other twenty were evaluated. Predominant parenchymal patterns were categorized into consolidation, ground glass opacity (GGO), and mixed patterns. Distribution of parenchymal abnormalities was assessed.
Results: Median age was 46.5 years. The CURB-65 score, which is the scoring system for severity of community acquired pneumonia, had a median of 1. Median duration of symptoms was 3 days. All had abnormal chest x-ray findings. The median number of days after the hospital visit that Chest CT was performed was 1. The reasons for chest CT performance were radiographic findings unusual for pneumonia (n=13) and unexplained dyspnea (n=7). GGO was the most predominant pattern on CT (n=13, 65.0%). Parenchymal abnormalities were observed in both lungs in 13 cases and were more extensive in the lower lung zone than the upper. Central and peripheral distributions were identified in ten and nine cases, respectively. One showed diffuse distribution. Peribronchial wall thickening was found in 16 cases. Centrilobular branching nodules (n=7), interlobular septal thickening (n=4), atelectasis (n=1), pleural effusion (n=5), enlarged hilar and mediastinal lymph nodes (n=6 and n=7) were also noted.
Conclusion: Patchy and bilateral GGO along bronchi with predominant involvement of lower lungs are the most common chest CT findings of pandemic influenza A/H1N1 pneumonia.

Key Words: Influenza A Virus, H1N1 Subtype; Tomography, X-Ray Computed; Pandemics; Pneumonia; Influenza, Human

Introduction

A novel 2009 pandemic influenza A/H1N1 virus was identified as a cause of human respiratory disease in Mexico and the United States[1,2]. Its rapid spread throughout the world led to prompting of the World Health Organization to declare a pandemic in June 2009[3]. As of March 2010, more than 213 countries worldwide, and overseas territories or communities have reported laboratory confirmed cases of a novel pandemic influenza A/H1N1, including at least 16,713 deaths[4].

Clinical manifestations of pandemic influenza A/H1N1 viral infection include fever, cough, sore throat, chills, headache, rhinorrhea, shortness of breath, myalgia, arthralgia, fatigue, vomiting, or diarrhea. These symptoms are usually mild and the clinical course is

Address for correspondence: **Yee Hyung Kim, M.D.**
Department of Pulmonary and Critical Care Medicine, Kyung Hee University Hospital at Gangdong, Kyung Hee University, 149, Sangil-dong, Gangdong-gu, Seoul 134-727, Korea
Phone: 82-2-440-6281, Fax: 82-2-440-8150
E-mail: yeehyung@naver.com
Received: Nov. 16, 2010
Accepted: Jan. 16, 2011

known to be self-limiting in most patients. However, cases of lethal illness, such as severe pneumonia or acute respiratory distress syndrome, have been reported, even in previously healthy persons[5].

It is essential that clinicians be able to recognize possible causes of pandemic influenza A/H1N1 viral infection in patients with newly developed pneumonic infiltration, so that the appropriate diagnostic tests can be ordered and specific therapy can be provided as early as possible. Until now, chest CT findings of novel pandemic influenza A/H1N1 viral pneumonia have only been documented in a few reports[6-10]. Most of these studies enrolled a small number of cases from western countries. One study analyzing the largest number of patients included cases that were presumed, not confirmed, as having pandemic influenza A/H1N1 viral infection[9]. Additionally, one study performed in Korea included cases regardless of bacterial co-infection[6], and other studies have demonstrated the probability of bacterial co-infection. Due to limitations of previous data, we reviewed chest CT findings of confirmed novel pandemic influenza A/H1N1 viral pneumonia in the Korean population.

Materials and Methods

Approval for this study was obtained from the Institutional Review Board of Kyung Hee University Hospital at Gangdong (KHNMC IRB 2010-020). Because it was a retrospective study, informed consent was waived. From October 2009 to Februrary 2010, 3,621 patients in two university-affiliated hospitals were diagnosed as respiratory infection due to novel pandemic influenza A/H1N1 virus by reverse transcriptase polymerase chain reaction (RT-PCR). Ninety seven patients were admitted due to severe symptoms. Pneumonia associated with influenza A/H1N1 was identified in 56 cases. A confirmed case of pure pandemic influenza A/H1N1 viral pneumonia is defined as a person with flu-like symptoms, newly developed pneumonic infiltration on chest radiography, and positive response of RT-PCR for pandemic influenza A/H1N1 virus without evidence of other microbial infection. Among 56 patients with influenza A/H1N1 viral pneumonia, chest CT was performed in 22 patients. Two patients co-infected with bacteria were excluded. Therefore, this study finally included 20 cases.

Respiratory samples were initially collected, processed, and tested according to the guidelines of the Centers for Disease Control and Prevention[11]. Chest radiographs were obtained using conventional radiography in the posteroanterior and/or lateral projection on the day when patients visited the emergency department or were admitted. Chest CT scans were performed on Brilliance 16- and 64-slice CT scanners (Philips Medical Systems, Best, The Netherlands) or Lightspeed 16 slice CT scanners (GE, Milwaukee, USA) with 16×0.75 mm or 64×0.625 mm collimation, 120 kVp tube voltage, 150 mAs effective tube current, and 0.5 seconds per rotation time. Dose modulation was applied during CT data acquisition. CT images were obtained from the lung apex to the adrenal gland during on breath-hold obtained at the end of inspiration. Intravenous contrast material was administered for eight CT examinations. MDCT images were obtained within 2 days after initial chest radiography. One radiologist with thoracic imaging experience of 7 years reviewed all of the images with both mediastinal (width 295 HU; level 50 HU) and parenchymal (width 1,500 HU; level −700 HU) window settings.

Lung parenchyma was classified as normal or abnormal on chest radiography. CT scans were analyzed for the presence and distribution of parenchymal abnormal findings, such as consolidation and ground glass opacity (GGO). According to the definition of the Fleischer society[12], GGO was defined as hazy areas of increased opacity or attenuation without obscuration of the underlying vessels, and consolidation was defined as homogenous opacification of parenchyma with obscuration of underlying vessels.

Predominant parenchymal patterns on chest CT were categorized into three: consolidation, GGO, and mixed pattern. Dominant distribution of parenchymal abnormalities was also assessed: bilateral or unilateral, cen-

tral, peripheral or diffuse, and peribronchial or not. Evaluation of lung parenchymal abnormality was performed for the four slices, including aortic arch level (level I), tracheal bifurcation level (level II), left inferior pulmonary vein level (level III), and supradiaphragmatic level (2 cm above right diaphragm dome, level IV). Each slice was subjectively assessed and graded separately, according to the percentage showing parenchymal abnormal findings. A score of 0 was assigned if there was no abnormality; a score of 1 was given if less than 25% of lung parenchyma showed abnormal findings; a score of 2, 3, or 4 was assigned when abnormal finding involved 25～50%, 50～75%, or more than 75%, respectively, of lung parenchyma. Additional findings, including bronchial wall thickness, centrilobular branching nodules, interlobular septal thickening, atelectasis, pleural effusion, pericardial effusion, enlarged lymph node, and pulmonary thromboembolism were evaluated. Stastistical analysis was performed using SPSS version 12.0 (SPSS Inc., Chicaco, IL, USA). The data were expressed as the median and interquatile range (IQR, 25 to 75th percentiles) or mean±standard deviation. To assess the relationship between variables, Spearman bivariate correlation analysis was used. $p < 0.05$ was considered statistically significant.

Results

Demographic and clinical characteristics are summarized in Table 1. Patients included 13 men and 7 women with a median age of 46.5 years (IQR, 18～69.7). Seven patients had preexisting medical conditions, including hypertension (n=3), diabetes mellitus (n=2), ischemic heart disease (n=2), cerebrovascular disease (n=2), chronic lung disease (n=2), valvular heart disease (n=1), malignancy (n=1), and ulcerative colitis (n=1). Median duration of symptoms prior to hospital visit was median 3 days (IQR, 1～4.75). Cough, sputum, and exertional dyspnea were found in most patients. Other manifestations included sore throat (n=8), nausea (n=6), diarrhea (n=3), and pleuritic pain (n=3). Supplemental oxygen was required for nine patients; however, most patients did not need mechanical ventilation or management in the intensive care unit except one. The median score for CURB-65 (confusion, blood urea nitrogen >19 mg/dL, respiratory rate ≥ 30 breaths/min, systolic blood pressure <90 mm Hg or diastolic blood pressure <60 mm Hg, and age ≥ 65 years. Each risk factor scores one point, for a maximum score of 5, which reflects the severity of community-acquired pneumonia (CAP), was 1 (IQR, 0～1.75). These baseline characteristics

Table 1. Demographic characteristics in 20 patients with novel pandemic influenza A/H1N1 viral pneumonia

Age, yr	46.5 (IQR, 18～69.7)
Male	13 (65.0)
Non-smoker	10 (50.0)
Immunocompromised host	1 (5.0)
Number of patients with chronic diseases	7 (35.0)
Days from symptoms onset to hospital visit	3 (IQR, 1～4.75)
Number of patients requiring oxygen supplement	9 (45.0)
Number of patients requiring mechanical ventilator	0 (0.0)
Number of case requiring ICU admission	1 (5.0)
Duration of hospitalization, day	7 (IQR, 4～10)
Score of CURB-65*	1 (IQR, 0～1.75)
Number of patients with abnormal chest x-ray	20 (100)

Data are presented as median (IQR) or number (%).
*Score of CURB-65 is an acronym for each of the risk factors measured (confusion, blood urea nitrogen 19 mg/dL or greater, respiratory rate of 30 breaths per minute or greater, systolic blood pressure less than 90 mm Hg, or diastolic blood pressure 60 mm Hg or less, and age 65 or older). Each risk factor scores one point, for a maximum score of 5.
IQR: interquartile range.

Table 2. Chest CT features in 20 patients with novel pandemic influenza A/H1N1 viral pneumonia

Predominant patterns	
Ground glass opacity	13 (65.0)
Consolidation	5 (25.0)
Mixed	2 (10.0)
Distributions	
Bilateral	13 (65.0)
Central vs. Peripheral vs. Diffuse	10 (50.0) vs. 9 (45.5) vs. 1 (5.0)
Mean total score of extent of lesion*	3.57±1.46
Zonal involvement†	
Level I	6 (0.4±0.5)
Level II	10 (0.7±0.5)
Level III	15 (1.0±0.6)
Level IV	19 (1.6±0.6)
Bronchial wall thickness*	
None	4 (20.0)
<1/2 of PAT‡	9 (45.0)
1/2≤PAT<1	7 (35.0)
Additional findings	
Centrilobular braching nodules	7 (35.0)
Interlobular septal thickening	4 (20.0)
Atelectasis	1 (5.0)
Pleural effusion	5 (25.0)
Enlarged hilar lymph node	6 (30.0)
Enlarged mediastinal lymph node	7 (35.0)

Values are presented as number (%) unless otherwise indicated. *Evaluation of bronchial wall thickness and extent of lesion was available in 19 patients, since one had dense consolidation with atelectasis in the left upper lobe, †aortic arch level (level I), tracheal bifurcation level (level II), left inferior pulmonary vein level (level III), and supradiaphragmatic level (2 cm above right diaphragm dome, level IV). Data were presented as number of cases (mean score of extent of lesion), ‡peribronchial artery thickness.

had no significant differences compared with those of 34 patients who was diagnosed of pandemic influenza A/H1N1 pneumonia, but only chest x-ray was taken from.

Initial chest radiographic images obtained on the day patients visited the emergency department or were admitted were abnormal in all cases. Chest CT was performed on median 1 day (IQR, 0～2) from the day when initial chest radiographs were obtained. The reasons for chest CT performance were radiographic findings unusual for pneumonia (n=13) and unexplained dyspnea (n=7), compared with extent of involvement in chest radiograph. Table 2 shows chest CT features by pandemic influenza A/H1N1 viral pneumonia. GGO was the most predominant pattern on CT (n=13, 65.0%) (Figures 1, 2). Consolidation and mixed pattern were dominant in five and two patients, respectively. Need for oxygen supplements was not correlated with dominancy of GGO (r=−0.23, p=0.391).

Parenchymal abnormalities were observed on both lungs in 13 cases (65.0%). Central (n=10, 50%) and peripheral (n=9, 45.0%) distribution of these were identified at a similar rate. One patient had a diffuse lesion in the right lower lobe (Figure 3). Parenchymal abnormalities were more extensive in the lower lung zone. Most patients had pneumonic infiltration below the left inferior pulmonary vein (level III) (Figure 3). In contrast, only 6 patients had pneumonic infiltration above the aortic arch (level I). Mean scores given in each level per patient were 0.4±0.5 in level I and 0.7±0.5 in level II, whereas those of level III and IV were 1.0±0.6 and 1.6±0.6, respectively. The extent of involvement had no significant correlation with duration of hospital stay. Most patients (n=16, 80.0%) had bronchial wall thickening, which was less than thickness of peribronchial artery. A trend of negative correlation was observed between age and bronchial wall thickness (r=−0.488, p=0.065).

Additional CT findings were as follows: centrilobular branching nodules (n=7, 35.0%), interlobular septal thickening (n=4, 20.0%), atelectasis (n=1, 5.0%), pleural effusion (n=5, 25.0%), enlarged hilar lymph node (n=6, 30.0%), and enlarged mediastinal lymph node (n=7, 35.0%). Pulmonary thromboembolism was not noted on eight contrast-enhanced chest CT scans.

All patients received antimicrobial treatment, including olsetamivir, at the time of suspicion of pandemic influenza A/H1N1 viral pneumonia, without laboratory confirmation. All patients finally survived. Follow-up chest radiographs were obtained on median 13.5 (IQR, 10.25～15.75) days from the day when initial chest radiographs were obtained. Initial parenchymal abnormalities were resolved completely, except in 2 patients with residual infiltration.

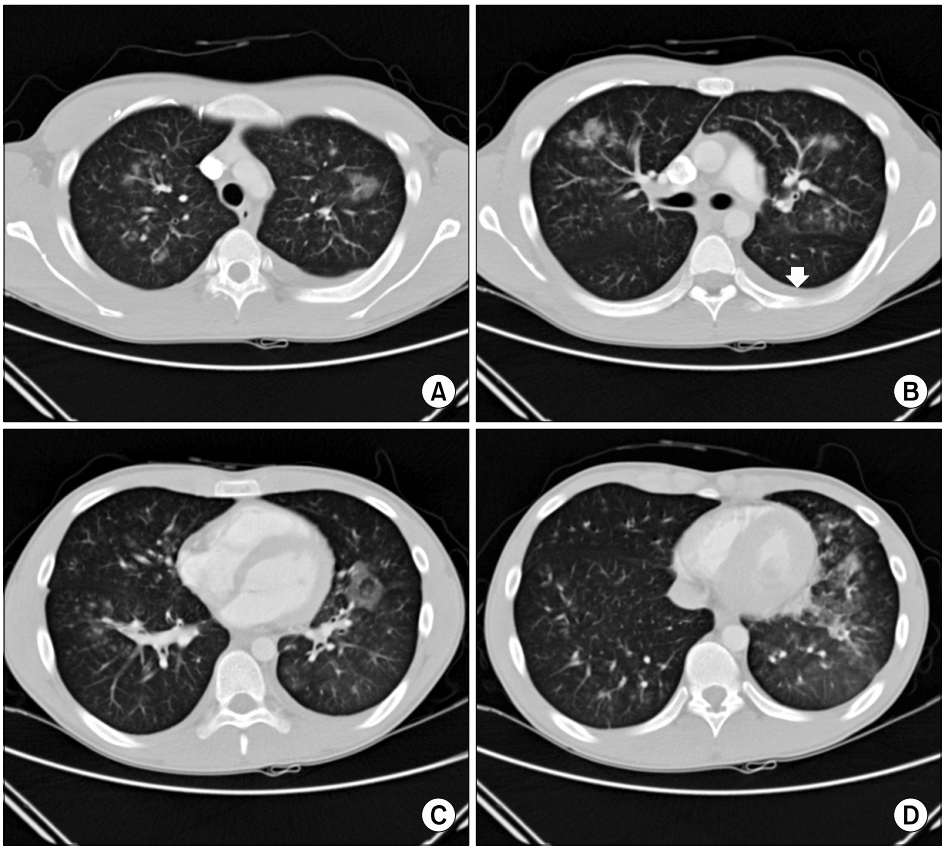

Figure 1. An 18-year-old male patient with pandemic influenza A/H1N1 pneumonia. Chest CT scans obtained in the level I (A), level II (B), level III (C) and level IV (D) showed bilateral and multi-focal ground glass opacities. Left pleural effusion was also found (white arrow). CT: computed tomography.

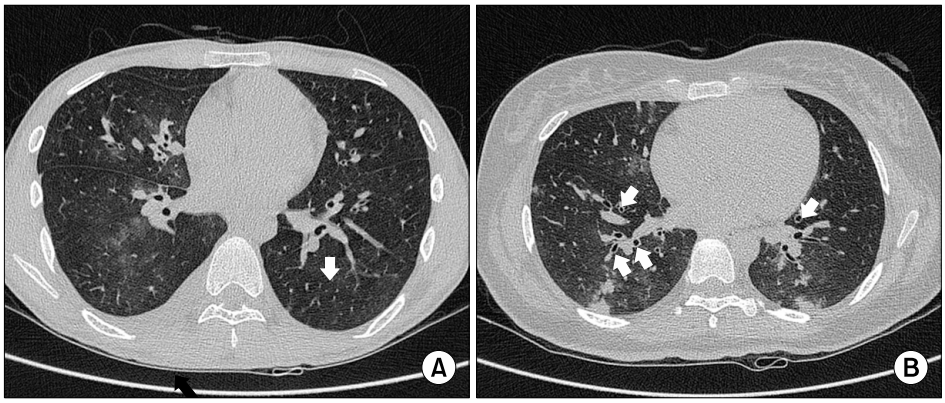

Figure 2. A 27-year-old male (A) and a 42-year-old female (B) with pandemic influenza A/H1N1 pneumonia. Chest CT revealed that multiple ill-defined ground glass opacities in middle to lower lungs with bronchial wall thickening (A, B) (white arrow). Right pleural effusion was also seen (A) (black arrow). CT: computed tomography.

Discussion

Influenza virus infection usually involves the upper respiratory tract, including the trachea and major bronchi. However, type A and occasionally type B organisms can cause influenza viral pneumonia[13]. Recently, novel pandemic influenza A/H1N1 virus, more commonly known as swine flu, was first reported in Mexico, and, as of late 2009, has become the current dominant strain[5,14]. Fatal cases leading to death have been reported, even in healthy persons, and pneumonia was one of the main causes of hospitalization and death[5,15].

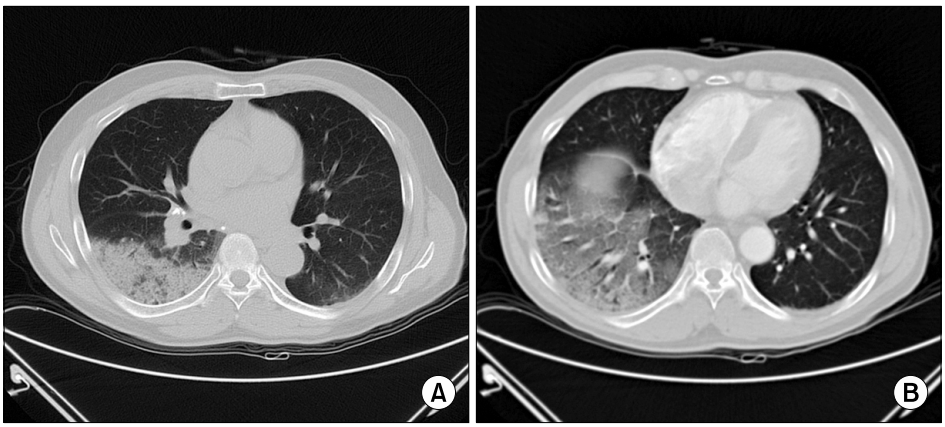

Figure 3. A 55-year-old male patient with pandemic influenza A/H1N1 pneumonia. Chest CT obtained 4 days after onset of symptoms showed a diffuse mixed pattern with ground glass opacities and consolidation in the right lower lobe. CT: computed tomography.

Therefore, recognition of the possibility of pandemic influenza A/H1N1 viral pneumonia is important.

We attempted to evaluate chest CT findings of pandemic influenza A/H1N1 pneumonia. In our study, patchy central or peripheral GGO, peribronchiolar distribution with bronchovascular bundle thickening, and predominant involvement of both lower lung zones were the most common CT findings of pandemic influenza A/H1N1 viral pneumonia. These findings seem not to be so different from those of previous studies from western countries[5,7-9]. However, some differences were observed. Observation of pulmonary embolism on CT was reported in five cases involving patients who required ICU admission and mechanical ventilation in a previous study[9]. However, there was no such case in our study. In addition, patchy consolidation was the most predominant finding in one study[9]. And a retrospective study of 108 patients younger than 20 years who had microbiologically confirmed pandemic influenza A/H1N1 viral infection and available initial chest radiographs showed that bilateral consolidation was the predominant radiological finding in patients with a more severe clinical course, whereas prominent peribronchial marking with hyperinflation was observed in children with a mild and self-limited clinical course[16]. However, our study and several previous studies revealed that GGO was the most predominant parenchymal abnormality[7,8]. These radiological differences from previous studies might be attributed to demographic characteristics, such as age and disease severity. In general, 3 or more of CURB-65 score was regarded as severe CAP. The patients included in our study did not have 3 or more of CURB-65 score. Therefore, it might be reasonable that pulmonary thromboembolism was absent, or that consolidation was less prominent than GGO in our study. In addition, recent report showed that initial chest radiographic findings helped to predict patient outcome[17]. However, this study did not suggest that the score of extent of radiological involvement was correlated with duration of hospital stay. This might also be attributed to clinical features and small number of population included in this study.

Chest CT scan is superior to radiography in showing the distribution of the disease. RT-PCR is known to be more sensitive than antigen detection for influenza A virus by pharyngeal swab[18,19]. To describe the radiological findings of pandemic influenza A/H1N1 viral pneumonia more accurately, we selected patients who were confirmed by RT-PCR (microbiological) and chest CT (radiological). Additionally, we tried to rule out the possibility of infection due to other viruses and bacteria, since CT findings of bacterial co-infection might differ from those of pure pandemic influenza A/H1N1 viral pneumonia. According to our institutional protocol, the following examinations have been routinely performed in patients who were assumed to have CAP; sputum or pleural effusion gram stain/culture, blood culture, sputum acid fast bacilli smear/culture, IgM and IgG to *Mycoplasma pneumoniae* and/or *Chlamydophila pneumoniae*, and antigen of *Streptococcus pneumoniae* and

Legionella pneumophilia type I in urine. Multiplex PCR of pharyngeal secretion have been selectively performed for detection of respiratory viruses, including influenza virus, parainfluenza virus, pneumometavirus, respiratory syncytial virus (RSV), adenovirus, and rhinovirus. Our institutional protocol for CAP covers a broader spectrum of microbiologic etiology than that of recommendations of ATS/IDSA[20]. Through our microbial evaluation, two among 22 patients who were diagnosed with pandemic influenza A/H1N1 viral pneumonia were identified as being co-infected with bacteria (One patient co-infected with *Streptococcus pneumoniae* died of respiratory failure, and the other was co-infected with *Haemophilus influenzae* and finally recovered.). They were finally ruled out from analysis. Therefore, we think that our study analyzed cases that were not co-infected with other microbial organisms, although all causative organisms were not identified by microbial examination.

Radiographic findings in viral pneumonia on chest CT, as well as chest radiograph, appear to be variable and overlapping. A recent study with a small number of cases showed that there were no significant differences in individual CT features of community-acquired viral pneumonia, including influenza virus, adenovirus, RSV, and parainfluenza virus[21]. Also, to the best of our knowledge, there have been no data showing a comparison of radiological findings of pandemic influenza A/H1N1 viral pneumonia with those of other viral pneumonia. Since our study is also not comparative study, we could not suggest the remarkable findings of pandemic influenza A/H1N1 viral pneumonia, comparing with other viral pneumonia. Therefore further study should be performed for clarification of differences between community-acquired viral pneumonias, including pandemic influenza A/H1N1 viral pneumonia.

We acknowledge several limitations of our study. First, this is a retrospective study and includes a small number of cases. Most of the patients in our current study did not need ICU care. Therefore, there is a possibility that the analysis was biased toward patients with relatively less severe forms of the disease. We think that this limitation influenced negative effect on correlation of radiological extent with hospital stay. Second, this study was also not comparative, and so we were not able to make a conclusion as to whether there were differences from other community-acquired viral pneumonia or not. Third, this study did not include 36 patients with pandemic influenza A/H1N1 pneumonia whom chest CT scan was not obtained from. In addition, two patients with sputum positive bacterial culture (*S. pneumoniae* and *H. influenzae*) were finally excluded according to purpose of this study. Predominant CT finding of them was consolidation. Therefore the findings of this study may not represent the feature of CT in pandemic influenza A/H1N1 pneumonia.

In conclusion, patchy and bilateral GGO along bronchovascular bundles with predominant involvement of lower lung zones in non-severe pandemic influenza A/H1N1 viral pneumonia are the most common chest CT features. Also, it seems that bronchial wall thickness has a trend of negative correlation with age. When these radiological findings are observed on chest CT scan, the possibility of pandemic influenza A/H1N1 viral pneumonia can be considered, based on clinical information such as community outbreaks, age, symptom onset and duration, and severity of disease.

Acknowledgements

All the authors have no source of financial support or conflict of interest in connection with this paper.

Author Contributions

Yee Hyung Kim was the primary investigator and corresponding author who performed collecting and analyzing all the clinical and radiological data. He also made a draft of the manuscript and revised it with interpretation of data; *Jun Seong Son* was the primary investigator who analyzed the clinical data; *Young Kyung Lee* reviewed the radiological images of all patients; *Cheon Woong Choi, Myung Jae Park, Jee-Hong Yoo, Hong Mo Kang and Jong Hoo Lee* were revising the

manuscript.

References

1. Centers for Disease Control and Prevention (CDC). Update: swine influenza A (H1N1) infections--California and Texas, April 2009. MMWR Morb Mortal Wkly Rep 2009;58:435-7.
2. Centers for Disease Control and Prevention (CDC). Swine influenza A (H1N1) infection in two children--Southern California, March-April 2009. MMWR Morb Mortal Wkly Rep 2009;58:400-2.
3. New influenza A (H1N1) virus: global epidemiological situation, June 2009. Wkly Epidemiol Rec 2009;84:249-57.
4. World Health Organization. Global alert and response (GAR): pandemic (H1N1) 2009-update 91 [Internet]. Geneva: World Health Organization; 2010 [cited 2008 Mar 18]. Available from: http://www.who.int/csr/don/2010_03_12/en/.
5. Perez-Padilla R, de la Rosa-Zamboni D, Ponce de Leon S, Hernandez M, Quiñones-Falconi F, Bautista E, et al. Pneumonia and respiratory failure from swine-origin influenza A (H1N1) in Mexico. N Engl J Med 2009;361:680-9.
6. Lee CW, Seo JB, Song JW, Lee HJ, Lee JS, Kim MY, et al. Pulmonary complication of novel influenza A (H1N1) infection: imaging features in two patients. Korean J Radiol 2009;10:531-4.
7. Mollura DJ, Asnis DS, Crupi RS, Conetta R, Feigin DS, Bray M, et al. Imaging findings in a fatal case of pandemic swine-origin influenza A (H1N1). AJR Am J Roentgenol 2009;193:1500-3.
8. Ajlan AM, Quiney B, Nicolaou S, Müller NL. Swine-origin influenza A (H1N1) viral infection: radiographic and CT findings. AJR Am J Roentgenol 2009;193:1494-9.
9. Agarwal PP, Cinti S, Kazerooni EA. Chest radiographic and CT findings in novel swine-origin influenza A (H1N1) virus (S-OIV) infection. AJR Am J Roentgenol 2009;193:1488-93.
10. Marchiori E, Zanetti G, Hochhegger B, Mauro Mano C. High-resolution CT findings in a patient with influenza A (H1N1) virus-associated pneumonia. Br J Radiol 2010;83:85-6.
11. World Health Organization. Global alert and response (GAR): CDC protocol of realtime RTPCR for influenza A (H1N1) [Internet]. Geneva: World Health Organization; 2009 [cited 2008 Mar 18]. Available from: http://www.who.int/csr/resources/publications/swineflu/realtimeptpcr/ en/index.html.
12. Hansell DM, Bankier AA, MacMahon H, McLoud TC, Müller NL, Remy J. Fleischner Society: glossary of terms for thoracic imaging. Radiology 2008;246:697-722.
13. Nolan TF Jr, Goodman RA, Hinman AR, Noble GR, Kendal AP, Thacker SB. Morbidity and mortality associated with influenza B in the United States, 1979-1980. A report from the Center for Disease Control. J Infect Dis 1980;142:360-2.
14. Centers for Disease Control and Prevention (CDC). Surveillance for the 2009 pandemic influenza A (H1N1) virus and seasonal influenza viruses - New Zealand, 2009. MMWR Morb Mortal Wkly Rep 2009;58:918-21.
15. Donaldson LJ, Rutter PD, Ellis BM, Greaves FE, Mytton OT, Pebody RG, et al. Mortality from pandemic A/H1N1 2009 influenza in England: public health surveillance study. BMJ 2009;339:b5213.
16. Lee EY, McAdam AJ, Chaudry G, Fishman MP, Zurakowski D, Boiselle PM. Swine-origin influenza a (H1N1) viral infection in children: initial chest radiographic findings. Radiology 2010;254:934-41.
17. Aviram G, Bar-Shai A, Sosna J, Rogowski O, Rosen G, Weinstein I, et al. H1N1 influenza: initial chest radiographic findings in helping predict patient outcome. Radiology 2010;255:252-9.
18. Centers for Disease Control and Prevention (CDC). Evaluation of rapid influenza diagnostic tests for detection of novel influenza A (H1N1) Virus - United States, 2009. MMWR Morb Mortal Wkly Rep 2009;58:826-9.
19. Drexler JF, Helmer A, Kirberg H, Reber U, Panning M, Müller M, et al. Poor clinical sensitivity of rapid antigen test for influenza A pandemic (H1N1) 2009 virus. Emerg Infect Dis 2009;15:1662-4.
20. Mandell LA, Wunderink RG, Anzueto A, Bartlett JG, Campbell GD, Dean NC, et al. Infectious Diseases Society of America/American Thoracic Society consensus guidelines on the management of community-acquired pneumonia in adults. Clin Infect Dis 2007;44(Suppl 2):S27-72.
21. Shiley KT, Van Deerlin VM, Miller WT Jr. Chest CT features of community-acquired respiratory viral infections in adult inpatients with lower respiratory tract infections. J Thorac Imaging 2010;25:68-75.